Rotavirus assembly – interaction of surface protein VP7 with middle layer protein VP6

J. M. Gilbert[1,*], **N. Feng**[1], **J. T. Patton**[2], and **H. B. Greenberg**[1]

[1]Stanford University School of Medicine, Division of Gastroenterology and Department
of Microbiology and Immunology and the Palo Alto V. A. Health Care System,
Palo Alto, California, U.S.A.
[2]National Institute of Allergy and Infectious Disease, Bethesda, Maryland, U.S.A.

Summary. The interaction between the rotavirus proteins viral protein 6 (VP6) and VP7 was examined in several exogenous protein expression systems. These proteins associated in the absence of other rotaviral proteins as demonstrated by a coimmunoprecipitation assay. Deletion analysis of VP7 indicated that truncations of either the mature amino or carboxyl terminus disrupted the proper folding of the protein and were not able to coimmunoprecipitate VP6. Truncation analysis of VP6 indicated that trimerization of VP6 was necessary, but not sufficient, for VP7 binding. MAb mapping and coimmunoprecipitation interference assays indicate that the VP6 amino acid residues between 271 and 342 are required for VP7 interaction. The interaction of VP6 and VP7 was also examined by the assembly of soluble VP7 onto baculovirus-expressed virus-like particles containing VP2 and VP6. Abrogation of this binding by preincubation of the particles with VP6 MAbs mapped to this same domain of VP6, validated our coimmunoprecipitation results. VP6 IgA MAbs that have been shown to be protective in vivo, but not a nonprotective IgA MAb, can interfere with VP7 binding to VP6. This suggests that these IgA MAbs may protect against rotavirus infection by blocking rotavirus assembly.

Introduction

Rotavirus, a member of the *Reoviridae*, is a major cause of severe gastroenteritis in young children and cause substantial mortality and morbidity worldwide [15,

*Present address: Harvard Medical School, Department of Pathology, 200 Longwood Ave. Armenise 233, Boston, MA 02115, U.S.A.

23]. Rotavirus particles are non-enveloped and consist of a segmented, double-stranded RNA genome, the RNA-dependent RNA polymerase VP1 and the guanylyl transferase VP3 [4, 25, 30] and are surrounded by a layer of VP2 protein. This layer is subsequently encompassed by VP6, the most abundant rotaviral protein which comprises 51% of the total virus protein [28]. VP6 forms trimers [17, 32, 36] which are thought to associate with the cores during viral assembly. Epitopes exposed on the VP6 trimers also determine the subgroup (SG) specificity of the viral particle (SG I, SG II, SG I/II or SG non I/II; [18, 20]). The VP6 middle layer is then surrounded by a sheath of VP7, a glycoprotein, with the dimeric viral attachment protein, VP4, extending out from the surface [9].

The replication and packaging of the dsRNA genome into double-layered particles consisting of VP2 and VP6, occurs rapidly in cytoplasmic viroplasms [31, 34]. VP4 is expressed as a soluble protein in the cytoplasm and VP7 is cotranslationally inserted into the membrane of the endoplasmic reticulum (ER) [9]. How these two proteins assemble on to the double-layered particle to form the complete triple-layered particle is not known. It is thought that assembly is assisted by the nonstructural protein NSP4, a cytoplasmic-facing ER-resident protein which binds to VP6 on the double-layered particles [29]. The double-layered particle/NSP4 complex buds into the ER, along with VP4, with which it is somehow associated [9]. The specific mechanism by which the lipid envelope is shed from the double-layered particle, how NSP4 dissociates, and how the mature triple-layered particle is formed from the components is not understood. It is clear that major rearrangements must occur, one of the most significant ones is the enveloping of the VP6 encased double-layered particle with a layer of VP7.

Cryoelectron microscopic data [32, 37] indicates that in the mature rotaviral particle, VP6 interacts with VP2, and VP4, and VP7, on diametrical faces of VP6. Since there appears to be a significant amount of interaction between VP6 and VP7 within the mature particle, we investigated whether we could define the interactive domains of these two proteins in the absence of any other rotaviral proteins. Mapping these domains of VP6 and VP7 will aid in our understanding of the assembly processes of rotavirus. Although virus-like particles consisting of VP6 and VP7 can be produced from recombinant baculoviruses [33, 35], we chose to examine the interaction between VP6 and VP7 using a transient system that allows rapid analysis of many mutants. Here we present data, employing a combination of biochemical and molecular techniques, indicating that although the VP6 interaction domain of VP7 appears to be complex, the VP7 interaction domain on VP6 resides or depends upon amino acid residues 271 to 328.

Materials and methods

Cells and viruses

Baby hamster kidney cells (BHK), were maintained in Dulbecco's modified Eagle's medium (DMEM; Biowhittaker; Walkersville, MD) with 4.5 g per 1 glucose containing 10% fetal bovine serum (FBS; Hyclone; Logan, UT), 100 IU per ml penicillin, 100 IU per ml streptomycin, 0.29 mg per ml L-glutamine (Irvine Scientific, Santa Ana, CA), and 0.25 mg per

ml amphotericin B (LifeTechnologies; Gaithersburg, MD) in a 5% CO_2 incubator at 37 °C. Vaccinia virus expressing the T7 polymerase and the plasmid pTM1 were gifts of B. Moss (Laboratory of Viral Diseases, National Institute of Allergy and Infectious Disease, Bethesda, MD USA).

Spodoptera frugiperda 9 (Sf-9) cells were grown in monolayer culture with Sf-900 II protein-free media (LifeTechnologies) supplemented with 100 IU per ml penicillin, 100 IU per ml streptomycin, 0.29 mg per ml L-glutamine and 2.5% FBS 27 °C. Recombinant baculovirus stocks (VP2 and VP6 of the RF virus strain; gift of J. Cohen, Laboratorie de Virologie et Immunologie Moleculaires INAS, Jousy-en Josas, France) were grown in Sf-9 cells in Sf-900 II media supplemented with 60 IU per ml of penicillin and streptomycin, and 0.17 mg per ml of L-glutamine.

Recombinant DNA

Wild-type rhesus rotavirus (RRV) strain VP7 (referred to as wt RRV VP7), is a full length cDNA of the tissue culture adapted RRV strain; the cDNA for tissue culture adapted, wild-type RF strain VP6 (referred to as wt RF VP6) was a gift of D. Poncet (Laboratorie de Virologie et Immunologie Moleculaires INAS, Jousy-en Josas, France). The ability of the VP6 and VP7 proteins of these two different strains has been shown by the formation of baculovirus expressed virus-like-particles [5, 13].

For optimal expression in the vaccinia virus T7 polymerase infection/transfection system (described below), the start ATGs of all VP6 and VP7 cDNAs were altered to an Nco I site (ccATGg) and subcloned into the vector pTM1 Nco I site to take advantage of an IRES [11, 12]. For creation of amino terminal truncations from wt RF VP6, the new start codons were created by mutating the desired sequence to a new Nco I site and these constructs were subcloned into the pTM1 vector. The mature, amino terminal truncations derived from wt RRV VP7 were created by introduction of a second Pfl MI site, at the desired location, downstream from the endogenous site. Excision of the Pfl MI fragment and religation of the deleted vector resulted in deletions 3′ distal to the native, signal sequence cleavage site. For the production of carboxyl terminal truncations from the wt RF VP6 and wt RRV VP7 cDNAs, a stop codon was co-inserted with an Xba I site at the indicated locations. All cDNA plasmids were purified using a Qiagen kit (Qiagen; Santa Clarita, CA). Site-directed mutagenesis was performed as described by Kunkel et al. [24] and the mutations were confirmed by sequencing on an ABI automated DNA sequencer.

Antibodies and immunoprecipitations

The VP7 antibodies used were the neutralizing monoclonal antibodies (MAbs) against the RRV strain 159, 4C3, 5H3, and 4F8 [27, 38] and the non-neutralizing, cross-reactive MAbs 60 (raised against the RRV strain) and 129 (raised against the WA strain; [38]). The two VP6 immunoglobulin G (IgG) MAbs used were 255/60 (SGI; [19]) and 5E6 [1]. The VP6 IgA MAbs are as described in Burns et al. [1]. Rabbit hyperimmune serum (R2, raised against RRV) was also used [2]. The amount of IgG and IgA MAbs used for VP6 immunoprecipitations was determined by ELISA [10]. For immunoprecipitations, IgG MAbs were precoupled to Protein A-Sepharose (Sigma; St. Louis, Mo.) for 2 h at 4 °C. IgA MAbs were precoupled to goat anti-mouse IgA biotin (Kirkegaard and Perry; Gaithersburg MD) and avidin agarose (Pierce Chemical Company; Rockford, IL) for 2 h at 4 °C. The antibody-bead complexes were washed twice with lysis buffer (see below), added to the ^{35}S-labelled protein and the samples were immunoprecipitated overnight at 4 °C. Samples were washed [21] and then subjected to sodium dodecyl sulfate polyacrylamide gel electrophoresis (SDS-PAGE) as described below. For MAb blocking experiments, ^{35}S labelled samples were incubated with

the individual IgA MAbs of equivalent ELISA titer for 1 h at room temperature. Samples were then immunoprecipitated with IgG MAbs as described above.

Sodium dodecylsulfate polyacrylamide gel electrophoresis (SDS PAGE)

Samples were processed for SDS-PAGE as described [14] and electrophoresed at the indicated acrylamide concentrations (Novex; San Diego, CA). For fluorography, the gels were fixed, enhanced with Entensify (Dupont; Boston, MA), dried and then exposed to film (X-OMAT; Eastman-Kodak; Rochester, NY). All figures were scanned using a UMAX scanner model #UC1260. The figures were prepared using Adobe Photoshop and Canvas programs.

Protein expression

For expression of ^{35}S-labelled proteins for immunoprecipitation, the vaccinia virus T7 DNA polymerase infection/transfection system was used [11, 12]. Briefly, confluent wells of BHK cells in 6 well dishes were infected with the recombinant vaccinia virus at a multiplicity of infection (moi) of 2.5 for 1 h at 37 °C in a CO_2 incubator. Cells were then transfected with the desired cDNAs with LipofectAmine (LifeTechnologies) and incubated for 5 h at 37 °C in a CO_2 incubator. Cells were washed and then starved in media lacking cysteine and methionine (LifeTechnologies) for 30 min. Cells were labelled with 50 μCi per ml ^{35}S Translabel (ICN; Irvine, CA) for 1.5 h at 37 °C in a CO_2 incubator. Cells were washed with phosphate buffered saline and triturated off the plates. Cells were pelleted at $1000 \times$**g** for 3 min, lysed in lysis buffer (HEPES-buffered saline containing 0.1% NP-40, 2.5 mM $CaCl_2$ and the following protease inhibitors: 0.1 M phenylmethyl sulfonyl fluoride, 1 μg per ml pepstatin A, 2 μg per ml leupeptin, 4 μg per ml aprotinin, 10 μg per ml antipain, 0.4 mM benzamidine, 10 μg per ml soybean trypsin inhibitor, and 0.5 mM iodoacetamide [Sigma Chemical Company; St. Louis, MO]) on ice for 15 min and pelleted at $14000 \times$**g** for 10 min at 4 °C. The ^{35}S lysates were examined by immunoprecipitation and coimmunoprecipitations as described below. Lysates of VP7 were deglycosylated by treatment with Endoglycosidase F (Boehringer Mannheim; Indianapolis, IN) according to the manufacturer's instruction.

For expression of VP6 proteins for trimer formation analysis, the in vitro transcription/translation system, TNT, was used (Promega; Madison, WI) according to the manufacturer's instructions. After translation, half the sample was incubated with denaturing SDS-PAGE loading buffer (0.5% SDS, 50 mM dithiothreitol) for 5 min at 100 °C. The other half was incubated in a nondenaturing loading buffer for 5 min at room temperature. Samples were then subjected to SDS-PAGE and fluorography as described above.

VLP production

Double-layered virus-like particles, containing RF VP2 and VP6, were prepared as described previously [13]. Briefly, monolayers of cells were infected with the recombinant baculoviruses at a moi of 5 in Sf-900 II media. After incubation for 24–36 h at 27 °C, the inoculum was removed by aspiration, and media containing the protease inhibitors pepstatin, aprotinin, and leupeptin (0.5 μg per ml; Sigma) were added. These protease inhibitors were added daily until the cells were harvested at four to five days post-infection. Particles were purified and analysed as described in Crawford et al. [5]. The protein concentration of the CsCl-purified 2/6 VLPs was determined using the Pierce BCA Protein Reagent Kit (Pierce).

For the VP7/double-layered VLP binding assay, 20 μg CsCl purified 2/6 VLPs were preincubated or not with IgA or IgG MAbs against VP6, of equivalent ELISA titer, for 2 h at 4 °C. These VLPs complexed with antibodies were incubated with a lysate of 5×10^5 BHK

cells expressing ^{35}S labelled VP7 at 25 °C for 90 min. Samples were then pelleted through an equal volume of 35% (wt per vol) sucrose in lysis buffer at 100,000×**g** for 2.5 h at 4 °C in a TLA 45 rotor (Beckman Instruments, Inc.; Fullerton, CA). The tubes were harvested into top, sucrose and pellet fractions and resuspended in lysis buffer of a volume equal to the top and sucrose fractions. The samples were then immunoprecipitated with MAb 60, and subjected to SDS-PAGE and fluorography as described above.

Results

Co-immunoprecipitation of VP6 and VP7 with VP7 MAbs

The ability of the rotavirus structural proteins to interact has been previously examined on a preliminary level using both reassortant rotaviruses and baculovirus expressed rotavirus virus-like-particles [8, 9, 33, 35]. We initially observed that VP6 and VP7 could be coimmunoprecipitated from cell lysates of rotavirus infected cells as well as cells infected with recombinant vaccinia viruses expressing both wild-type VP6 and VP7 (data not shown). To begin to characterize potential interactions between VP6 and VP7 on a molecular level, we examined whether an immunoprecipitable complex could form between VP6 and VP7 when expressed in a heterologous system. Using the vaccinia virus T7 infection/transfection expression system [11, 12], BHK cells were co-transfected with the individual plasmids encoding wt RF VP6 and wt RRV VP7 alone. These proteins from two different strains are known to interact about as well as wild-type as shown in both reassortant studies as well as with VLPs [5, 8, 13]. Cells were incubated at 37 °C, radiolabelled and harvested as described in the Methods section and cell lysates were prepared. The lysates were incubated with a series of VP7 MAbs, 60, 129, 159, 4C3, 4F8, and 5H3. The MAbs efficiently precipitated VP7 and when VP6 and VP7 were present together in the lysate, all MAbs could bring down VP6 along with VP7 (Fig. 1). The VP7 MAbs did not recognize VP6 when it was expressed alone (Fig. 1). The coimmunoprecipitation of VP6 by VP7-directed MAbs was specific for the VP7 MAbs, since treatment of the same lysates with MAbs against VP6 only precipitated VP6 and did not coimmunoprecipitate VP7 (data not shown). Cells that were infected with the recombinant vaccinia virus that were either transfected with the parental pTM1 or untransfected cells, did not immunoprecipitate any radiolabelled proteins with any of the antibodies used (data not shown). The VP6 and VP7 proteins did not need to be expressed together within the same cell to form a complex. Mixing detergent lysates from cells that were transfected with either individual cDNA (wt RF VP6 or wt RRV VP7) still resulted in the VP6/VP7 complex formation (data not shown). Additionally, the levels of either wt RF VP6 or wt RRV VP7 expressed were due to individual transfection efficiencies and had little effect on the apparent efficiency of coimmunoprecipitation. Additionally, using different subgroups and G types of VP6 and VP7 showed that this interaction could be recapitulated and is not dependent upon either the subgroup specific epitopes of VP6 or the G type determinants of VP7, similar to what is seen with genetic reassortants (data not shown).
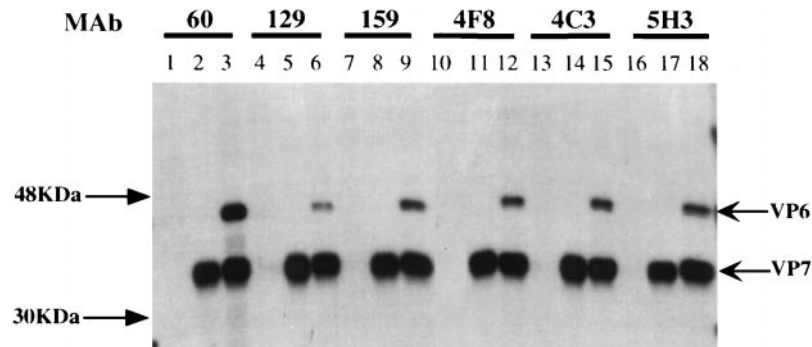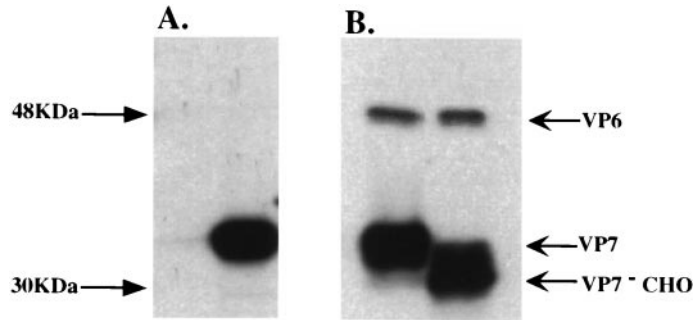
Fig. 1. Coimmunoprecipitation of wt RF VP6 with wt RRV VP7. BHK cells were transfected with the cDNAs encoding wt RF VP6 and wt RRV VP7, or wt RRV VP7 alone and cells were labelled with ^{35}S methionine and cysteine. Cells were harvested, lysed and proteins examined by immunoprecipitation and subjected to sodium dodecyl sulfate polyacrylamide gel electrophoresis (SDS-PAGE, 12% acrylamide; Novex, San Diego, Calif.) as described previously (Gilbert and Greenberg, 1997). The lanes are labelled as MAb 60 (*1–3*), MAb 129 (*4–6*), MAb 159 (*7–9*), MAb 4F8 (*10–12*), MAb 4C3 (*13–15*) and MAb 5H3 (*16–18*). For each MAb, the first lane is the wt RF VP6 lysate alone, the middle lane is the wt RRV VP7 lysate alone and the third lane is the wt RF VP6 and wt RRV VP7 lysates together. The migration positions of wt RF VP6 and wt RRV VP7 are as indicated on the right and molecular mass are as indicated to the left

Analysis of VP7 and the interaction with VP6

The mature conformation of VP7 requires the presence of calcium [6–8]. To determine whether the calcium-bound form of VP7 is the only form of VP7 that can interact with VP6, radiolabelled cell lysates containing RF VP6 and RRV VP7 were prepared in lysis buffer in the absence of calcium. The samples were immunoprecipitated with either MAb 159, which recognizes a calcium-dependent epitope of VP7, or MAb 60, which can recognize VP7 in the absence of calcium [6, 7]. As expected, MAb 159 did not immunoprecipitate any protein since there was no calcium present and, although MAb 60 immunoprecipitated VP7, no VP6 was coimmunoprecipitated (Fig. 2A). This is not due to a nonspecific effect on VP6 in the absence of calcium since VP6 is immunoprecipitated and does form trimers in the absence of calcium (data not shown). This finding indicates that VP6 only binds to the calcium-bound form of VP7.

During rotaviral replication, VP7 is translocated into the endoplasmic reticulum (ER) where the signal sequence is cleaved and carbohydrate residues are added. VP7 is retained within the ER until the rotaviral double-layered particle buds into the ER where the final viral maturation takes place. We next examined whether complete glycosylation of VP7 is required for its interaction with VP6. BHK cells were transfected with either wt RF VP6 or wt RRV VP7. Cells were labelled, harvested and lysates prepared. The wt RRV VP7 lysate was treated or not with Endoglycosidase F to remove high mannose, asparagine-linked sugars. The treated and untreated wt RRV VP7 containing lysates were incubated with wt RF VP6 containing lysates and then immunoprecipitated with MAb 60. VP6

Fig. 2. A Coimmunoprecipitation of wt RF VP6 with wt RRV VP7 in the absence of calcium. BHK cells were transfected with the cDNAs for wt RF VP6 and wt RRV VP7. After labelling, lysates were prepared in absence of calcium and were immunoprecipitated with MAb 159 (lane 1) or MAb 60 (lane 2). Samples were processed as described in the legend to Fig. 1. The migration positions of wt RF VP6 and wt RRV VP7 are as indicated on the right; molecular mass is indicated on the left. **B** Coimmunoprecipitation of wt RF VP6 with wt RRV VP7 in the absence of high mannose, N-linked glycosylation. BHK cells were transfected with the cDNAs for either wt RF VP6 or wt RRV VP7. Cells were labelled and lysates were prepared. The wt RRV VP7 containing lysate was either treated or not with Endoglycosidase F and then incubated with the lysate containing wt RF VP6. Samples were immunoprecipitated and examined by SDS-PAGE and fluorography as described in the Methods section and the legend to Fig. 1. Lane 1 contains the untreated wt RRV VP7 sample, lane 2 contains the deglycosylated wt RRV VP7 sample. The migration positions of wt RF VP6 and wt RRV VP7 are as indicated on the right; molecular mass is indicated on the left

associated with VP7 regardless of the glycosylation status of VP7 (Fig. 2B) indicating that N-acetyl-glucosamine residues are not required for the VP6/VP7 interaction.

We next investigated if there was a specific domain of VP7 that was involved in binding to VP6. A series of carboxyl terminal truncations, as well as two deletions 3′ to the signal sequence cleavage site, of wt RRV VP7 were constructed using specific site-directed mutagenesis [24]. The mutant proteins were expressed in BHK cells and lysates were immunoprecipitated with rabbit hyperimmune sera (against RRV) and were determined to be expressed at approximately equal levels (Table 1). Although all the VP7 mutants were expressed, only the two most carboxyl terminal VP7 truncations (Δ 275–326 and Δ 289–326) and the most amino terminal VP7 truncation (Δ 58–87) were immunoprecipitated by the non-neutralizing MAb 60 (Table 1).

To further characterize the VP7 truncation mutants, we examined the ability of the mutant proteins to be precipitated by several conformation-dependent neutralizing antibodies. The lack of immunoprecipitation with the neutralizing MAbs 159, 5H3 [27], 4F8, and 4C3 [38] indicated that these calcium-dependent, conformationally defined neutralization epitopes on VP7 were not maintained in any of the truncations (Table 1). The three VP7 truncations that could be precipitated by MAb 60 (Δ 275–326, Δ 289–326, and Δ 58–87) were co-transfected into BHK

Table 1. Amino and carboxyl terminal truncations of TC-adapted wt RRV VP7. BHK cells were transfected with the cDNAs for either wt RRV VP7 or mutant RRV VP7 and the immunoprecipitability by either rotavirus hyperimmune serum (*R2*) or a series of VP7 monoclonal antibodies is indicated. The defined monoclonal antibody epitope (if known) is indicated in parentheses. The ability of these same VP7 constructs to coimmunoprecipitate wt RF VP6 with MAb 60 is also as indicated

VP7 construct	Immunoprecipitations						CoIP of VP6
	$R2^a$	60	159 $(a^2\ 94)^b$	5H3 $(a^2\ 211)$	4F8 $(a^2\ 96)$	4C3 $(a^2\ 94)$	
wt RRV VP7	+	+	+	+	+	+	+
Δ 58–87	+	+	−	−	−	−	−
Δ 58–101	+	−	−	−	−	−	ND
Δ 245–326	+	−	−	−	−	−	ND
Δ 275–326	+	+	−	−	−	−	−
Δ 289–326	+	+	−	−	−	−	−

[a]Hyperimmune serum or VP7 monoclonal antibody used;
[b]Amino acid epitope of antibody

cells with wt VP6 and their coimmunoprecipitation phenotype was compared with wt VP7. Surprisingly, although these mutants were recognized by MAb 60, they were not able to coimmunoprecipitate VP6 (Table 1) indicating that the truncated VP7 proteins either could not bind VP6 or this interaction was no longer stable enough to be maintained under the coimmunoprecipitation conditions. The loss of immunoprecipitability of these truncation mutants by the specific MAbs of defined epitopes correlated with the loss of interaction and coimmunoprecipitation with VP6 and prevented us from localizing the domain of VP7 involved in VP6 binding.

Analysis of VP6 and the interaction with VP7

We next examined if there was a specific domain of VP6 that was involved in binding to VP7. A series of amino terminal and carboxyl terminal VP6 truncations were constructed using specific site-directed mutagenesis. The mutant VP6 proteins were expressed in BHK cells and immunoprecipitation with rabbit hyperimmune sera indicated that all the mutants were expressed (Table 2) although the Δ 271–396 was expressed at a lower level (or is less immunoreactive) than the other mutants. Wild-type RF VP6 and the VP6 truncations were co-transfected into BHK cells along with wt RRV VP7 and their ability to be coimmunoprecipitated was examined. Although all the amino terminal truncations could be coimmunoprecipitated with VP7 by MAb 60, deletions of the carboxyl terminus greater than 53 amino acids (mutants Δ 271–396, Δ 311–396 and Δ 328–396) resulted in a loss of coprecipitation (Table 2). This would indicate that the VP7 binding region, or minimum proper folding domain, of VP6 is located between amino acid residues 125 and 343.

Table 2. Amino and carboxyl terminal truncations of wt RF VP6. BHK cells were transfected with the cDNAs for either wt RF VP6 or mutant RF VP6 and the immunoprecipitability by either rotavirus hyperimmune serum (*R2*) or a series of VP6 monoclonal antibodies is indicated. The antibody isotype is indicated in parentheses. The ability of these same VP6 constructs trimerize and to be coimmunoprecipitated with VP7 using MAb 60 is also indicated

	Immunoprecipitations						Trimerization	CoIP
VP6 construct	R2[a]	255/60 (SGI) (IgG)[b]	5E6 (IgG)	7D9 (IgA)	10C10 (IgA)	8D3 (IgA)		
wild-type VP6	+	+	+	+	+	+	+	+
Δ 1–49	+	+	+	+	+	+	+	+
Δ 1–63	+	+	+	+	+/−	+	+	+
Δ 1–125	+	+	+	−	−	−	+	+
Δ 271–396	+/−	−	−	−	−	−	−	−
Δ 311–396	+	−	+	−	−	−	−	−
Δ 328–396	+	+	+	−	−	+	+	−
Δ 343–396	+	+	+	−	+	+	+	+

[a]Hyperimmune serum or VP6 monoclonal antibody used;
[b]Immunoglobulin isotype

The inability to form a complex with VP7 did not appear to correlate with trimerization of VP6. Wild-type and mutant VP6 proteins were expressed in an in vitro transcription/translation system (TNT; Promega). Samples were boiled in SDS samples buffer or not treated and then examined by SDS-PAGE and fluorography for trimer formation. Similar to what was seen by Clapp and Patton [3], only the carboxyl terminal truncations greater than 68 amino acids (mutants Δ 271–396 and Δ 311–396) lost the ability to form trimers (Table 2). Therefore, since the mutant Δ 328–396 can form trimers but cannot be coprecipitated, trimerization would appear to be necessary but not sufficient for the interaction of VP6 with VP7.

Immunoprecipitation of VP6 truncations

To more precisely define the VP7 interaction domain of VP6, we examined the ability of a series of VP6 IgG and IgA MAbs to immunoprecipitate the VP6 truncations. 255/60 is a subgroup I specific MAb (SGI) with a complex binding epitope that has been localized to residues 296–299 and 305 [39]. 5E6 is an IgG MAb raised against the murine EC virus that recognizes subgroup I, subgroup II and non I/non II VP6 proteins. The VP6 IgA MAbs (7D9, 10C10 and 8D3) described in Burns et al. [2], recognize subgroup I, subgroup II and non I/non II VP6 proteins. The IgA MAbs 7D9 and 10C10 can protect mice from rotavirus in vivo (when present as circulating IgA from a backpack tumor [2]) whereas 8D3 can not protect from rotavirus infection in this model. None of these IgG or IgA MAbs can neutralize rotavirus in a standard in vitro neutralization assay [2].

The truncated VP6 proteins were expressed in BHK cells and lysates were immunoprecipitated with MAbs (Table 2). Immunoprecipitation data indicated that none of the MAbs could precipitate the Δ 271–396 mutant, only MAb 5E6 recognizes the Δ 311–396 mutant, and none of the IgA MAbs recognize the Δ 1–125 mutant (Table 2). In addition, all of the carboxyl terminal truncations eliminated the immunoprecipitation of VP6 by the protective IgA MAb 7D9.

From the immunoprecipitation data it appears that several of the MAbs bind to similar epitopes. To determine whether there are overlapping epitopes between the different MAbs we examined whether the IgA MAbs could interfere with the immunoprecipitation of wt RF VP6 by the VP6 IgG MAbs. VP6 protein was expressed in BHK cells and the lysates were incubated with the IgA MAbs. Samples were then immunoprecipitated with either 255/60 or 5E6 IgG MAbs precoupled
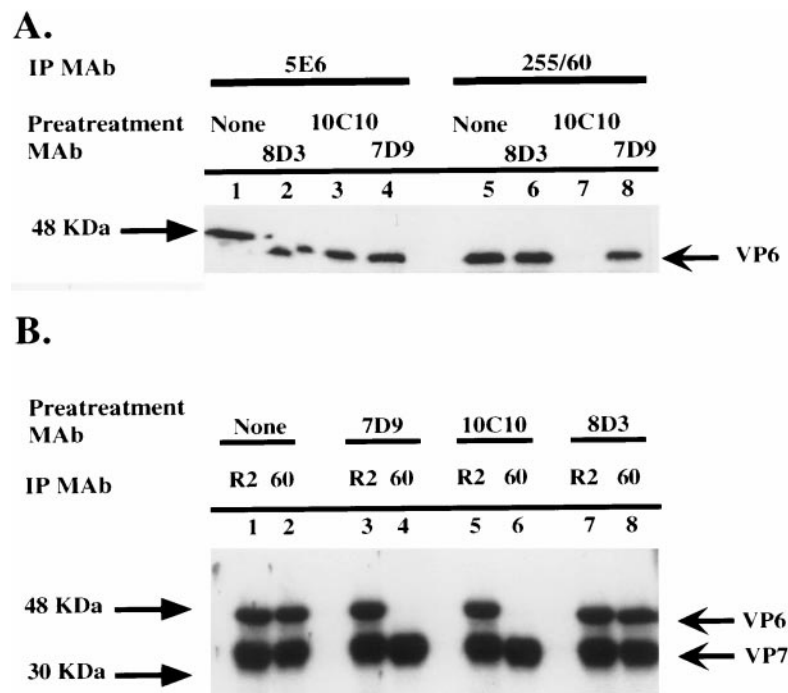
Fig. 3. A IgA blocking of wt RF VP6 immunoprecipitation. wt RF VP6 containing lysates were prepared as previously described. Samples were treated with no IgA MAb (*1, 5*), 8D3 (*2, 6*), 10C10 (*3, 7*) or 7D9 IgA MAbs (*4, 8*) and then immunoprecipitated with either 5E6 IgG MAb (*1–4*) or 255/60 IgG MAb (*5–8*). Samples were processed as described in the legend to Fig. 1. The migration position of wt RF VP6 is as indicated on the right; the molecular mass is indicated on the left. **B** IgA blocking of wt RF VP6 coimmunoprecipitation. Lysates were prepared containing wt RF VP6 and wt RRV VP7 as previously described. Samples were incubated with either no IgA MAb (*1, 2*), 7D9 (*3, 4*), 10C10 (*5, 6*) or 8D3 IgA MAbs (*7, 8*). Samples were then immunoprecipitated with either rabbit hyperimmune sera (odd numbered lanes) or MAb 60 (even numbered lanes). The immunoprecipitates were then processed as described in the legend to Fig. 1. The migration positions of wt RF VP6 and wt RRV VP7 are as indicated on the right; the molecular mass is indicated on the left

to Protein A Sepharose and examined by SDS-PAGE and fluorography (Fig. 3A). Neither 7D9 nor 8D3 IgA MAbs interfered with the immunoprecipitation of VP6 by the IgG MAbs but the IgA MAb 10C10 blocked the immunoprecipitation of VP6 by the subgroup I-specific 255/60 IgG MAb. This finding supports the notion that the VP6 epitope for the protective 10C10 IgA MAb overlaps or is affected by the epitope for subgroup I specific 255/60 IgG MAb. This binding site for 255/60 had previously been localized to include key amino acids at positions 296–299 and 305 [26, 39]. Interestingly, although there appears to be some overlap between the epitopes of MAbs 255/60 and 10C10, MAb 255/60 immunoprecipitates Δ 1–125 but 10C10 does not, indicating that the overlap and/or interaction is not complete.

IgA blocking of VP6 coimmunoprecipitation

Since VP6 MAbs recognize epitopes between amino acid residues 125 and 343 that may overlap with the VP7 interaction domain of VP6, we next examined whether the VP6 IgA MAbs could interfere with the coimmunoprecipitation of VP6 with VP7 via the IgG MAb 60. Lysates containing both radiolabelled RF VP6 and RRV VP7 prepared from BHK cells were preincubated with either no IgA MAb or 7D9, 10C10 or 8D3 IgA MAbs. Samples were then precipitated with either rabbit hyperimmune sera or the VP7 IgG MAb 60 and examined by SDS-PAGE and fluorography. As expected, without pretreatment with any IgA MAbs, VP6 is coprecipitated along with VP7 (Fig. 3B). Of the three IgA MAbs, only 8D3 did not interfere with the coimmunoprecipitation of VP6 with VP7 (Fig. 3B). The two VP6 IgA MAbs that neutralize rotavirus in the backpack model [2], 7D9 and 10C10, interfered with the coimmunoprecipitation (Fig. 3B). This observation supports the presumption that the MAb binding site of 7D9 and 10C10 are at, or interact with, the VP7 binding domain on VP6.

MAb blocking of VP7 assembly onto 2/6 VLPs

We were interested to determine whether the IgA-mediated prevention of the interaction between VP6 and VP7 could be extended to a system that is more like what is seen during rotaviral assembly. To this end, double-layered rotavirus-like particles (2/6 VLPs) were prepared from recombinant baculoviruses in Sf-9 cells. The CsCl purified particles were preincubated with either the VP6-specific IgA MAbs 10C10, 7D9 or 8D3, the VP6-specific IgG MAbs 255/60, 5E6, or not treated. After MAb binding, BHK cells lysates containing radiolabelled RRV VP7 were added to the particles and the samples further incubated as described in the methods section to allow VP7 assembly onto the particles. The particles containing radiolabelled VP7 were then separated from the soluble and any partially oligomerized VP7 by centrifugation over 35% sucrose and the presence of VP7 detected by immunoprecipitation with the VP7-specific MAb 60. VP7 incubated in buffer alone is retained in the top fraction, and some in the sucrose cushion after centrifugation (data not shown). After incubation with untreated 2/6 VLPs, the majority of the VP7 migrated with the pellet fraction (Fig. 4), indicating that

MAb
Pretreatment
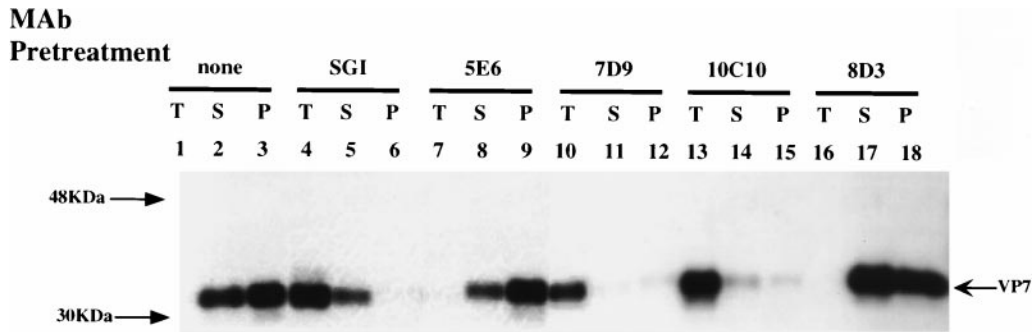
Fig. 4. MAb blocking of wt RRV VP7 assembly onto wt RF 2/6 VLPs. wt RF 2/6 VLPs were not treated or pretreated with MAbs 255/60, 5E6, 7D9, 10C10 or 8D3. Radiolabelled wt RRV VP7 containing lysates were added, incubated with the wt RF 2/6 VLPs and then particles were centrifuged through 35% sucrose as described in the Materials and Methods section. The samples were fractionated into top (*T*), sucrose (*S*), and pellet (*P*) fractions, and the samples were immunoprecipitated with the VP7-specific MAb 60. Samples were processed as described in the legend to Fig. 1. The markers for molecular mass are as indicated on the left

soluble VP7 had bound to the particles. VP7 also bound to the 2/6 VLPs preincubated with either 5E6 IgG MAb or IgA 8D3 MAb, the IgA that does not protect in vivo. Preincubation with either the subgroup specific, MAb 255/60 or the two IgA MAbs that were found to protect mice, 10C10 and 7D9, VP7 was found in the top fraction of the sucrose cushion (Fig. 4). This finding indicates that, similar to the immunoprecipitation results, these three antibodies, 255/60, 10C10 and 7D9 can each prevent the addition of VP7 to double-layered particles by binding at or near a region of VP6 necessary for the assembly of VP7.

Discussion

Given the extensive association of VP6 and VP7 within the assembled rotavirus particle, we thought it likely that these two proteins interacted directly without the requirement of the other rotaviral structural proteins. It has been clearly demonstrated with exogenous expression, from recombinant baculoviruses, of the rotaviral proteins, VP2, VP6 and VP7 in Sf-9 cells yields assembled particles [5]. This is thought to be analogous to the assembly that occurs in a natural rotaviral infection. VP6 is presented to VP7 in the context of a double-layered particle, with VP2. It is thought that the ER-localized VP7 is accessible for assembly due to the cytopathic effect of baculovirus infection. It has also been shown that virus-like particles containing only VP6 and VP7 can be expressed from recombinant baculoviruses [33, 35]. These particles were found in the media after full cytopathic effect had occurred but the mechanism of how VP6 and VP7 interact to assemble is not clear. In this paper we have used a combination of biochemical, immunological, and molecular techniques to examine the interaction between the two rotaviral structural proteins VP6 and VP7 in the absence of any other rotavirus proteins. With a rapid, transient protein expression system that uses an IRES

for efficient, high-level translation (the vaccinia virus T7 infection/transfection system [11, 12]) we could easily introduce and examine various mutations in VP6 and VP7 without the need to create recombinant baculoviruses. We initially established that both VP6 and VP7 were expressed and could be immunoprecipitated from NP-40 lysates with VP6- and VP7-specific MAbs, respectively (Fig. 1, Fig. 3, and data not shown). These antibodies only recognized their cognate rotavirus proteins as no endogenous proteins were immunoprecipitate from mock infected or vaccinia virus T7 infected cells (data not shown). Cotransfection and expression of the cDNAs for wild-type RF VP6 and wild-type RRV VP7 together resulted in association of the two proteins and this complex was demonstrated to be immunoprecipitable with MAbs to VP7 but not with MAbs to VP6 (Fig. 1 and data not shown). The reasons why the MAbs against VP6, that are not binding to the presumed VP7 binding site (8D3 and 5E6) cannot precipitate the VP6/VP7 complex are not clear. It could be that the interaction of the VP7-specific MAbs with VP7 are stable regardless of VP6 binding but that the binding of the VP6 MAbs to VP6 cause subtle changes in VP6 lowering the affinity of VP6 binding to VP7.

Since VP7 is a glycosylated, ER-resident protein, very little VP7 would be expected to be available to interact with soluble, cytoplasmic VP6, under normal circumstances. We only observed significant interaction by coimmunoprecipitation of wt RF VP6 along with wt RRV VP7 if the immunoprecipitations were performed in the presence of non-ionic detergent. If cells transfected with the cDNAs for both wt RF VP6 and wt RRV VP7 were instead disrupted by shear forces or hypotonic lysis, which leave the ER membranes intact, only low levels of RRV VP7 are precipitated from the soluble fraction. If RF VP6 is expressed in the same cell, very little RF VP6 is coimmunoprecipitated with wt RRV VP7, indicating that most, if not all VP7 is in the ER (data not shown). Separation of soluble and membraneous fractions confirmed that VP6 was in the soluble fraction and the vast majority of VP7 was contained in the membrane fraction. This is not unexpected as during virus assembly, VP6 and VP7 appear to interact only after the nascent double-layered particle buds into the ER.

During rotavirus replication, VP7 is an endoplasmic reticulum resident protein that is glycosylated and binds calcium ions. Whereas the high-mannose, asparagine-linked glycosylation of VP7 is not required for VP6 interaction (Fig. 2B), binding of calcium to VP7 and the formation of the proper VP7 conformation-dependent neutralization domain is required for VP6 association (Fig. 2A). Disruption of the VP6/VP7 interaction by the removal of CA^{2+}, as seen be loss of co-immunoprecipitability, may be analogous to what occurs when rotavirus enters cells and the change in Ca^{2+} concentration results in viral uncoating. A more detailed examination of the domain of VP7 that interacts with VP6 yielded little additional information; the mutated proteins could no longer interact with VP6. Retention of the mature calcium-dependent neutralizing epitopes of VP7 was a prerequisite for VP6 binding (Table 1) and that all the engineered truncations lost these epitopes. Even mutant proteins that could form oligomers similar to wild-type VP7 (data not shown) could not associate with VP6 if these

neutralization epitopes were lacking. This indicates that the mature conformation of VP7 is highly dependent upon both the amino and carboxyl terminal residues. Further analysis of the domain of VP7 that binds VP6 might benefit from additional structural data concerning VP7 or more quantitative studies of the interaction of VP6 with VP7 using chimeric or specific site-directed mutant VP7 molecules.

Examination of the VP7 interaction domain of VP6 proved more fruitful. Truncation analysis of VP6 indicated that, by coimmunoprecipitation assay, the VP7 interaction domain resided between amino acid residues 125 and 342 (Table 2). It also appears that the trimerization of VP6 is necessary, but not sufficient, for VP7 association as the VP6 mutant Δ 328–396 can trimerize but cannot be coimmunoprecipitated with VP7 (Table 2). The VP7 binding domain also appears to be within at least one of the VP2 binding regions of VP6 (residues 251–397; [3]). This would appear to contradict the cryoelectron microscopic data [32], which indicates that the mature quaternary structure of VP6 binds both VP2 and VP7, on opposite faces of VP6. A logical conclusion is that this region of VP6 is required for the proper folding of VP6 which can then trimerize and bind to the other constituent proteins of the mature rotavirus particle.

Epitope mapping of the VP6 truncations by immunoprecipitation indicated that several of the VP6-specific IgG and IgA MAbs appeared to bind at or near the putative VP7 binding domain (Table 2). Additionally, the IgG MAb 255/60 and the IgA MAb 10C10 appeared to overlap in their binding sites (Fig. 3A). Competition immunoprecipitation assays indicated that two of the three IgA MAbs (7D9 and 10C10) and one of the IgG MAbs (255/60) could block the ability of the complex between VP6 and VP7 to form (Fig. 3B). This epitope mapping data (Table 2) combined with previous data mapping the subgroup I epitope [39] would appear to indicate that the VP7 binding domain of VP6 lies between amino acid residues 271 and 342 or is highly dependent on these amino acid residues. Interestingly, this is a region of VP6 that is important for the ability to form stable trimers (residue 309; [3]) as well as near residues thought to be important for subgroup discrimination (residues 305 and 315; [16, 32, 39]). Again, from these data it is reasonable to assume that this domain of VP6 must fold into proper, stable conformation prior to VP7 binding.

By examining the binding of VP7 to VP6 in an environment that more closely resembles viral assembly, the binding of soluble VP7 proteins onto 2/6 VLPs, we were able to further define the region of VP6 to which VP7 may be binding. Two IgA MAbs (7D9 and 10C10) and the subgroup I specific IgG MAb (255/60) are able to block the binding of VP7 to the particles (Fig. 4). How VP7 can assemble on to particles that are bound with the two VP6 antibodies that cannot disrupt this interaction, 5E6 and 8D3, is not clear. VP6 epitope mapping data of the three MAbs that block VP7 binding to 2/6 VLPs indicates that the minimum region of VP6 that interacts with VP7 is between amino acid residues 271 and 328 of VP6. This reduced domain (271–328) is still within the larger region defined as important for VP2 binding (251–396), but may correspond to the outer face of VP6 where VP7 binds as opposed to the inner face where VP2 binds. Further

mutagenesis studies will be needed to identify individual amino acid residues directly involved in the binding of VP6 to VP7.

Interestingly the two IgA MAbs (7D9 and 10C10) that block the binding of VP7 to VP6, but not the IgA MAb that does not block binding (8D3), have been shown to protect mice from rotavirus infection in an in vivo backpack model. These blocking IgA MAbs do not neutralize intact rotavirus in standard neutralization assays which indicates that the corresponding epitopes are not accessible on the intact rotavirus particle. From these data it is enticing to speculate that these IgA MAbs neutralize rotavirus by blocking the assembly of VP6 onto VP7. The step in viral maturation where these IgA MAbs might disrupt the interaction between VP6 and VP7 is not clear. The double-layered particle, possibly associated with VP4, binds the receptor NSP4 which is located on the cytoplasmic face of the endoplasmic reticulum. The complex then buds into the endoplasmic reticulum where VP7 is retained, as it is associated with the lumenal face of the membrane. The transiently enveloped particle then completes the association and readjustment of the outer layer proteins, undergoes delipidation and turns into the mature rotavirus particle. If the double-layered particle interacts with the in vivo protective IgA MAbs prior to either budding into the endoplasmic reticulum or the postulated rearrangements of the proteins after budding, the interaction between VP6 and VP7 would be prevented. This would effectively inhibit rotavirus replication by inhibiting assembly. Other mechanisms of protection, such as inhibition of transcription, have not been ruled out, however. Further studies will be needed to determine when and where the IgA MAbs and the VP6 molecules interact in the infected cell.

Acknowledgements

References

1. Burns JW, Krishnaney AA, Vo PT, Rouse RV, Anderson LJ, Greenberg HB (1995) Analyses of homologous rotavirus infection in the mouse model. Virology 207: 143–153
2. Burns WB, Siadat-Pajouh M, Krishnaney AA, Greenberg HB (1996) Novel protective effect of rotavirus VP6 specific IgA monoclonal antibodies that lack conventional neutralizing activity. Science 272: 104–107
3. Clapp LL, Patton JT (1991) Domains in the major inner capsid protein essential for binding to single-shelled particles and for trimerization. Virology 180: 697–708
4. Cohen J, Lefevre F, Estes MK, Bremont M (1984) Cloning of bovine rotavirus (RF strain): nucleotide sequence of the gene coding for the major capsid protein. Virology 138: 178–182
5. Crawford SE, Labbe M, Cohen J, Burroughs MH, Zhou YJ, Estes MK (1994) Characterization of virus-like particles produced by the expression of rotavirus capsid proteins in insect cells. J Virol 68: 5915–5922

6. Dormitzer PR, Both GW, Greenberg HB (1994) Presentation of neutralizing epitopes by engineered rotavirus VP7's expressed by recombinant vaccinia viruses. Virology 204: 391–402
7. Dormitzer PR, Ho DY, Mackow ER, Mocarski ES, Greenberg HB (1992) Neutralizing epitopes on herpes simplex virus-1-expressed rotavirus VP7 are dependent on coexpression of other rotavirus proteins. Virology 187: 18–32
8. Estes MK (1996) Rotaviruses and their replication. In: Fields BN (ed), Fields virology. Lippincott-Raven, Philadelphia, pp 1625–1656
9. Estes MK, Cohen J (1989) Rotavirus gene structure and function. Microbiol Rev 53: 410–449
10. Feng N, Burns JW, Bracy L, Greenberg H (1994) Comparison of mucosal and systemic humoral immune responses and subsequent protection in mice orally inoculated with a homologous or a heterologous rotavirus. J Virol 68: 7776–7773
11. Fuerst TR, Earl PL, Moss B (1987) Use of a hybrid vaccinia virus-T7 RNA polymerase system for expression of target genes. Mol Cell Biol 7: 2538–2544
12. Fuerst TR, Niles EG, Studier FW, Moss B (1986) Eukaryotic transient-expression system based on recombinant vaccinia virus that synthesizes bacteriophage T7 RNA polymerase. Proc Natl Acad Sci USA 83: 8122–8126
13. Gilbert JM, Greenberg HB (1997) Virus-like particle induced fusion-from-without in tissue culture cells; role of outer-layer proteins VP4 and VP7. J Virol 71: 4555–4563
14. Gilbert JM, Hernandez LD, Chernov-Rogan T, White JM (1993) Generation of a water soluble oligomeric ectodomain of the Rous sarcoma virus envelope glycoprotein. J Virol 67: 6889–6892
15. Glass RI, Gentsch JR, Ivanoff B (1996) New lessons for rotavirus vaccines. Science 272: 46–48
16. Gorziglia M, Hoshino Y, Nishikawa K, Maloy WL, Jones RW, Kapikian AZ, Chanock RM (1988) Comparative sequence analysis of the genomic segment 6 of four rotaviruses each with a different subgroup specificity. J Gen Virol 69: 1659–1669
17. Gorziglia M, Larrea C, Liprandi F, Esparza J (1985) Biochemical evidence for the oligomeric (possibly trimeric) structure of the major inner capsid polypeptide (45K) of rotaviruses. J Gen Virol 66: 1889–1900
18. Greenberg HB, Flores J, Kalica AR, Wyatt RG, Jones R (1983a) Gene coding assignments for growth restriction, neutralization and subgroup specificities of the W and DS-1 strains of human rotavirus. J Gen Virol 64: 313–320
19. Greenberg HB, Valdesuso J, van Wyke K, Midthun K, Walsh M, McAuliffe V, Wyatt RG, Kalica AR, Flores J, Hoshino Y (1983b) Production and preliminary characterization of monoclonal antibodies directed at two surface proteins of rhesus rotavirus. J Virol 47: 267–275
20. Hoshino Y, Gorziglia M, Valdesuso J, Askaa J, Glass RI, Kapikian AZ (1987) An equine rotavirus (FI-14 strain) which bears both subgroup I and subgroup II specificities on its VP6. Virology 157: 488–496
21. Ishida S, Feng N, Tang B, Gilbert JM, Greenberg HB (1996) Quantification of the systemic and local immune responses to individual rotavirus proteins during rotavirus infection in mice. J Clin Microbiol 34: 1694–1700
22. Ito H, Minamoto N, Sasaki I, Goto H, Sugiyama M, Kinjo T, Sugita S (1995) Sequence analysis of cDNA for the VP6 protein of group A avian rotavirus: a comparison with group A mammalian rotaviruses. Arch Virol 140: 605–612
23. Kapikian AZ, Chanock RM (1996) Rotaviruses. In: Fields BN (ed) Fields virology. Lippincott-Raven, Philadelphia, pp 1657–1708

24. Kunkel TA, Roberts JD, Zakour RA (1987) Rapid and efficient site-specific mutagenesis without phenotypic selection. Methods Enzymol 154: 367–382
25. Liu M, Offit PA, Estes MK (1988) Identification of the simian rotavirus SA11 genome segment 3 product. Virology 163: 26–32
26. Lopez S, Espinosa R, Greenberg HB, Arias CF (1994) Mapping the subgroup epitopes of rotavirus protein VP6. Virology 204: 153–162
27. Mackow ER, Shaw RD, Matsui SM, Vo PT, Benfield DA, Greenberg HB (1988) Characterization of homotypic and heterotypic VP7 neutralization sites of rhesus rotavirus. Virology 165: 511–517
28. Mattion N, Gonzalez SA, Burrone O, Bellinzoni R, La Torre JL, Scodeller EA (1988) Rearrangement of genomic segment 11 in two swine rotavirus strains. J Gen Virol 69: 695–698
29. Meyer JC, Bergmann CC, Bellamy AR (1989) Interaction of rotavirus cores with the nonstructural glycoprotein NS28. Virology 171: 98–107
30. Patton JT, Jones MT, Kalbach AN, He YW, Xiaobo J (1997) Rotavirus RNA polymerase requires the core shell protein to synthesize the double-stranded RNA genome. J Virol 71: 9618–9626
31. Petrie BL, Greenberg HB, Graham DY, Estes MK (1984) Ultrastructural localization of rotavirus antigens using colloidal gold. Virus Res 1: 133–152
32. Prasad BV, Wang GJ, Clerx JP, Chiu W (1988) Three-dimensional structure of rotavirus. J Mol Biol 199: 269–275
33. Redmond MJ, Ijaz MK, Parker MD, Sabara MI, Dent D, Gibbons E, Babiuk LA (1993) Assembly of recombinant rotavirus proteins into virus-like particles and assessment of vaccine potential. Vaccine 11: 273–281
34. Richardson SC, Mercer LE, Sonza S, Holmes IH (1986) Intracellular localization of rotaviral proteins. Arch Virol 88: 251–264
35. Sabara M, Parker M, Aha P, Cosco C, Gibbons E, Parsons S, Babiuk LA (1991) Assembly of double-shelled rotaviruslike particles by simultaneous expression of recombinant VP6 and VP7 proteins. J Virol 65: 6994–6997
36. Sabara M, Ready KF, Frenchick PJ, Babiuk LA (1987) Biochemical evidence for the oligomeric arrangement of bovine rotavirus nucleocapsid protein and its possible significance in the immunogenicity of this protein. J Gen Virol 68: 123–133
37. Shaw AL, Rothnagel R, Chen D, Ramig RF, Chiu W, Prasad BVV (1993) Three-dimensional visualization of the rotavirus hemagglutinin structure. Cell 74: 693–701
38. Shaw RD, Vo PT, Offit PA, Coulson BS, Greenberg HB (1986) Antigenic mapping of the surface proteins of rhesus rotavirus. Virology 155: 434–451
39. Tang B, Gilbert JM, Matsui SM, Greenberg HB (1997) Comparison of the rotavirus gene 6 from different species by sequence analysis and localization of subgroup-specific epitopes using site-directed mutagenesis. Virology 237: 89–96

Author's address: Dr. H. B. Greenberg, P.A.H.C.S. 3401 Miranda Ave., MC 154C Building 101, Palo Alto, CA 9430, U.S.A.